HAL
open science

The oxyanion hole of Pseudomonas fluorescens mannitol 2-dehydrogenase: a novel structural motif for electrostatic stabilisation in alcohol dehydrogenase active sites

Mario Klimacek, B Nidetzky

To cite this version:

Mario Klimacek, B Nidetzky. The oxyanion hole of Pseudomonas fluorescens mannitol 2-dehydrogenase: a novel structural motif for electrostatic stabilisation in alcohol dehydrogenase active sites. Biochemical Journal, 2009, 425 (2), pp.455-463. 10.1042/BJ20091441 . hal-00479256

HAL Id: hal-00479256

https://hal.science/hal-00479256

Submitted on 30 Apr 2010

HAL is a multi-disciplinary open access archive for the deposit and dissemination of scientific research documents, whether they are published or not. The documents may come from teaching and research institutions in France or abroad, or from public or private research centers.

L'archive ouverte pluridisciplinaire **HAL**, est destinée au dépôt et à la diffusion de documents scientifiques de niveau recherche, publiés ou non, émanant des établissements d'enseignement et de recherche français ou étrangers, des laboratoires publics ou privés.

Biochemical Journal Immediate Publication. Published on 26 Oct 2009 as manuscript BJ20091441

The oxyanion hole of *Pseudomonas fluorescens* mannitol 2-dehydrogenase: a novel structural motif for electrostatic stabilisation in alcohol dehydrogenase active sites

Mario KLIMACEK and Bernd NIDETZKY[1]

Institute of Biotechnology and Biochemical Engineering, Graz University of Technology, Petersgasse 12/I, A-8010 Graz

[1] To whom correspondence should be addressed:

Dr. Bernd Nidetzky, Institute of Biotechnology and Biochemical Engineering, Petersgasse 12, Graz University of Technology, A-8010 Graz, Austria.

Phone: + 43-316-873-8400; Fax: + 43-316-873-8434; Email: bernd.nidetzky@tugraz.at

Running Title: The "oxyanion hole" of *Pseudomonas fluorescens* mannitol 2-dehydrogenase

THIS IS NOT THE VERSION OF RECORD - see doi:10.1042/BJ20091441

Accepted Manuscript

Licenced copy. Copying is not permitted, except with prior permission and as allowed by law.
© 2009 The Authors Journal compilation © 2009 Portland Press Limited

Abbreviations used. ADH, alcohol dehydrogenase; KIE, kinetic isotope effect; ^{D}KIE, primary deuterium kinetic isotope effect; ^{D_2O}KIE, solvent kinetic isotope effect; PfM2DH, D-mannitol 2-dehydrogenase from *Pseudomonas fluorescens*; PSLDRs, polyol-specifc long-chain dehydrogenase/reductase family of proteins

THIS IS NOT THE VERSION OF RECORD - see doi:10.1042/BJ20091441

Accepted Manuscript

Licenced copy. Copying is not permitted, except with prior permission and as allowed by law.
© 2009 The Authors Journal compilation © 2009 Portland Press Limited

SYNOPSIS

The side chains of Asn-191 and Asn-300 constitute a characteristic structural motif of the active site of *Pseudomonas fluorescens* mannitol 2-dehydrogenase that lacks precedent in known alcohol dehydrogenases and resembles the canonical oxyanion binding pocket of serine proteases. We have used steady-state and transient kinetic studies of the effects of varied pH and deuterium isotopic substitutions in substrates and solvent on the enzymatic rates to delineate catalytic consequences resulting from individual and combined replacements of the two asparagines by Ala. The rate constants for the overall hydride transfer to and from C2 of mannitol which were estimated as ~5×10^2 s^{-1} and ~1.5×10^3 s^{-1} in the wild-type enzyme, respectively, were selectively slowed, between 540 - and 2700-fold, in single-site mannitol 2-dehydrogenase mutants. These effects were additive in the corresponding doubly mutated enzyme, suggesting independent functioning of the two Asn residues in catalysis. Partial disruption of the oxyanion hole in single-site mutants caused an upshift, by ≥ 1.2 pH units, in the kinetic p*K* of the catalytic acid-base Lys-295 in the enzyme-NAD^+-mannitol complex. The oxyanion hole of mannitol 2-dehydrogenase is suggested to drive a precatalytic conformational equilibrium at the ternary complex level in which the reactive group of the substrate is "activated" for chemical conversion through its precise alignment with the unprotonated side chain of Lys-295 (mannitol oxidation) and C=O bond polarization by the carboxamide moieties of Asn-191 and Asn-300 (fructose reduction). In the subsequent hydride transfer step, the two Asn residues provide ~40 kJ/mol of electrostatic stabilisation.

Keywords: alcohol dehydrogenase, oxyanion hole, electrostatic stabilisation, polyol-specific long-chain dehydrogenases and reductases, stopped-flow kinetics, kinetic isotope effects, serine protease

THIS IS NOT THE VERSION OF RECORD - see doi:10.1042/BJ20091441

Accepted Manuscript

Licenced copy. Copying is not permitted, except with prior permission and as allowed by law.
© 2009 The Authors Journal compilation © 2009 Portland Press Limited

THIS IS NOT THE VERSION OF RECORD - see doi:10.1042/BJ20091441

INTRODUCTION

Stabilisation of partial negative charge formed on oxygen in intermediates or in the transition state of a chemical reaction is a common source of catalytic power in natural enzymes [1-7]. The particular task fulfilled in catalysis is often reflected by active-site preorganisation in the form of a so-called oxyanion hole [8]. A prototypical oxyanion-binding site is that of the serine protease chymotrypsin where two main-chain amide NH groups form hydrogen bonds with the oxygen atom on the substrate that develops the partial negative charge [5, 9, 10]. Structural characteristics of the chymotrypsin oxyanion hole are remarkably conserved in various enzymes spanning four EC classes [11-17] (see Supplementary Table S1). Despite fundamental differences in the chemical transformations catalysed, the reaction coordinates for these enzymes are usually united by the occurrence of a distinct, often tetrahedral, oxyanionic intermediate [5, 17-20]. Evolution of a common active-site structural motif would therefore seem to reflect the shared catalytic task of stabilising this intermediate. The proposed mechanism of aldehyde dehydrogenase, for example, proceeds through an anionic thiohemiacetal that is formed upon nucleophilic attack from the thiolate of a catalytic cysteine on the carbonyl carbon of the aldehyde substrate. This thiohemiacetal is subsequently oxidised to a thioester which decomposes hydrolytically to the acid product [18]. However, unlike aldehyde dehydrogenase and except in Zn-dependent alcohol dehydrogenases (ADH) [21-23], oxidation of an alcohol substrate by enzyme-bound $NAD(P)^+$ does not involve the clear intermediacy of an oxyanion species. The protease-like oxyanion-binding site in *Pseudomonas fluorescens* D-mannitol 2-dehydrogenase (PfM2DH) was therefore not anticipated. This site has no precedence in known ADHs and despite the striking similarity in geometric arrangement of the interacting groups, its role in the catalytic mechanism of PfM2DH cannot be inferred from well characterized oxyanion holes of other enzymes, some of which are listed in the Supplementary Table S1.

Catalytic features of the PfM2DH active site (Figure 1) are conserved in polyol-specific long-chain dehydrogenases/reductases (PSLDRs), a large family of metal-independent ADHs that function in microbial sugar metabolism [24, 25]. The three-dimensional structure of a ternary complex of PfM2DH bound to NAD^+ and mannitol showed the carboxamide groups of Asn-191 and Asn-300 within ≤ 3 Å distance to the reactive hydroxyl at carbon 2 of mannitol and the ε-amino group of Lys-295 (Figure 1) [16]. In the proposed mechanism of PfM2DH, Lys-295 functions as the catalytic base that facilitates hydride transfer to NAD^+ by (partial) proton abstraction from alcohol (Scheme 1A) [26]. Precise alignment of Lys-295 and the reactive 2-OH of the substrate is achieved through a conformational change that occurs at the level of the ternary complex and is observable as a kinetic isomerisation step (k_3 and k_4 in Scheme 1B) in rapid equilibrium [20, 26]. Lys-295 which has a pK of 9.2 in enzyme-NAD^+ becomes deprotonated, hence primed for catalysis in the precatalytic equilibrium (K_2 in Scheme 1B). Conversion of mannitol-bound PfM2DH into the enzyme form that reacts to give product (fructose) is therefore strongly pH-dependent. It is made irreversible above pH 10.0 due to deprotonation of the group comprising the unprotonated side chain of Lys-295 and the 2-OH of the substrate [20, 26].

Little is known about how the oxyanion holes of PfM2DH and related PSLDRs contribute to catalytic efficiency in enzymatic oxidoreduction of polyol and ketose substrates. Site-directed replacement of Asn-300 in PfM2DH by Ala resulted in partial kinetic unmasking of the hydride transfer step, suggesting an auxiliary role for the Asn in the chemical event of the overall transformation [27]. Using detailed analysis of kinetic consequences in this (N300A) and relevant further variants of PfM2DH, we have explored here the tasks fulfilled by Asn-191 and Asn-300 in the NAD(H)-dependent interconversion of mannitol and fructose catalyzed by the enzyme. Evidence is presented that electrostatic stabilization by the oxyanion hole does not only facilitate the catalytic step of hydride transfer but also "activates" the reactive groups on Lys-295 and mannitol in the preceding

Licenced copy. Copying is not permitted, except with prior permission and as allowed by law.
© 2009 The Authors Journal compilation © 2009 Portland Press Limited

Accepted Manuscript

conformational equilibrium. The triad of residues comprising Asn-191, Lys-295, and Asn-300 appear to fulfill a catalytic function in PfM2DH similar to that of Zn^{2+} in liver ADH [23, 28, 29].

EXPERIMENTAL

Materials and chemicals used, the preparation of enzymes, and details of the kinetic experiments are described under Supplementary Methods.

Site-directed mutagenesis, protein production and characterization

Mutations leading to substitutions of Asn-191 by Ala (N191A) or Leu (N191L) and both Asn-191 and Asn-300 by Ala (N191A-N300A) were introduced by using the inverse PCR protocol previously employed in constructing the gene for N300A [27]. The following oligonucleotide primers were used (mismatched bases are underlined): [5'-TGC GAT GCC CTG CCC CAC AAT-3'] for N191A; and [5'-TGC GAT CTC CTG CCC CAC AAT-3'] for N191L. The universal second primer had the sequence [5'-GGA CAT CAC GGT AAA CGC-3']. The primer encoding the substitution Asn-191→Ala and template plasmid carrying the gene for N300A were used in constructing the gene for N191A-N300A. DNA sequencing of entire genes was used to confirm that the desired mutation(s) had been introduced and no substitutions resulting from DNA polymerase errors had occurred.

Mutated genes were expressed in *E. coli* JM109 and recombinant proteins were purified to apparent homogeneity according to published protocols [30] (see Figure S1 in Supplementary Results). CD spectra and fluorescence emission spectra of isolated proteins were recorded using reported methods [27]. Dissociation constants for NAD^+ binding (K_{dNAD^+}) to wild-type and mutated enzymes were determined by fluorescence titration, as described elsewhere [27].

Steady-state kinetic analysis

Initial reaction rates were recorded spectrophotometrically at 25 °C, measuring the change in absorbance of NADH at 340 nm (ε_{340} = 6.22 $mM^{-1}cm^{-1}$) [20]. Apparent enzyme kinetic parameters (k_{cat}, $K_{substrate}$, $K_{coenzyme}$) were obtained from data recorded at varied substrate concentration as described elsewhere [20, 27, 30]. We use subscript O and R on k_{cat} to indicate mannitol oxidation (k_{catO}) and fructose reduction (k_{catR}), respectively.

The pH dependencies of kinetic parameters were determined in the pH range 5.2 – 10.5 for mannitol oxidation and 7.1 – 10.0 for fructose reduction. A three-component buffer, composed of MES, Tris and glycine, was used that displayed a pH-independent ionic strength of 0.1 M [31]. Kinetic isotope effects (KIE) that result from deuteration of substrate (2-[^{2}H]-mannitol; *S*-4-[^{2}H]-NADH) or solvent were determined using procedures described in a previous study of wild-type PfM2DH [20, 27, 30]. A nomenclature is used where superscript D describes the primary deuterium KIE and superscript D_2O describes the solvent KIE on the respective isotope-sensitive parameter [32]. ^{D}KIEs on kinetic constants for mannitol oxidation were obtained in the pH range 6.0 – 10.5.

Transient kinetic analysis

Stopped-flow kinetic experiments were performed as described elsewhere [20] using NADH absorbance (at 340 nm) to monitor the progress of the enzymatic reaction. The Applied Photophysics Reaction Analyser (model SX.18 MV) was equipped with a 20 μL flow cell (pathlength = 1 cm) and showed a dead-time of 1.5 ms under the conditions used. Each reaction was performed in at least seven repetitions. The resulting time courses were analysed as described in detail in the Supplementary Results. Enzyme was used in a concentration equal to or smaller than one-seventh of the concentration of the limiting substrate (for details, see Supplementary Methods). The levels of substrate and coenzyme were chosen to achieve a maximum degree of enzyme saturation (wild-type ≥ 75 %; mutants ≥ 63 %) in the steady state. Suitable controls were obtained by mixing reaction solutions lacking the enzyme.

Licenced copy. Copying is not permitted, except with prior permission and as allowed by law.
© 2009 The Authors Journal compilation © 2009 Portland Press Limited

THIS IS NOT THE VERSION OF RECORD - see doi:10.1042/BJ20091441

Accepted Manuscript

Proton release measurements were done using the pH indicator Phenol Red whose absorbance at 556 nm was recorded. Wild-type enzyme and N191L were gel-filtered twice to a 0.5 mM Tris/HCl buffer, pH 8.0, containing 3.2 μM Phenol Red, NAD^+ (wild-type: 3.0 mM; N191L: 20 mM) and NaCl such that the final ionic strength of this buffer was that of the reference (100 mM Tris/HCl, pH 8.0). The enzyme solution was rapidly mixed with a mannitol dissolved in the same buffer (wild-type enzyme: 200 mM; N191L: 260 mM). Proton concentrations were determined as described elsewhere [33].

Data fitting

Sigma Plot 2004 software (version 9.01) was used for non-linear least squares regression analysis. Eqn (1) describes pH dependencies where the activity ($Y = k_{cat}$, $k_{cat}/K_{substrate}$, k_{obs}) is constant at high pH and decreases below pK. C is the pH-independent value of Y at the optimum state of protonation. Eqn (2) describes a sigmoidal pH dependence with constant values of Y at high (C_H) and low pH (C_L). Eqn (3) describes a decrease of log$Y$ at low pH where the curve is flattened in the region of the apparent pK and therefore has a hollow appearance. There are three ionization constants (K) associated with this pH dependence provided that $pK_2 > pK_1 > pK_3$. ^{D}KIEs on k_{cat} and $k_{cat}/K_{substrate}$ were obtained from fits of Eqn (4) to the data [34]. E_V and $E_{V/K}$ are the isotope effects minus 1 on k_{cat} and k_{cat}/K_m, respectively, and F_i is the fraction of deuterium in the substrate or solvent.

$$\log Y = \log [C/(1+[H^+]/K)] \quad (1)$$
$$\log Y = \log [(C_H+C_L[H^+]/K)/(1+[H^+]/K)] \quad (2)$$
$$\log Y = \log \{C(1+[H^+]/K_1)/ [(1+[H^+]/K_2)(1+[H^+]/K_3)]\} \quad (3)$$
$$v=k_{cat}[E][S]/\{K_m(1+F_iE_{V/K})+[S](1+F_iE_V)\} \quad (4)$$

RESULTS

Properties of site-directed mutants

The spectroscopic signature of isolated PfM2DH mutants obtained by using CD and fluorescence was highly similar to that of the wild-type enzyme (see Figure S1 in Supplementary Results). NAD^+ binding affinity (K_{dNAD+}) was not strongly affected as result of the mutations (Table 1). Therefore, like N300A [27], the new mutants (N191A, N191L, N191A-N300A) appear to be correctly folded and retain a functional coenzyme binding site. Table 1 compares the different enzymes using apparent kinetic parameters determined under optimum pH conditions for oxidation (pH 10.0) and reduction (pH 7.1). Each single-site mutation as well as the combination of the two Ala substitutions in N191A-N300A caused a large decrease in $k_{cat}/K_{substrate}$ for either direction of the reaction, as compared to the corresponding catalytic efficiencies of the wild-type enzyme, by 3 and 7 orders of magnitude, respectively. Loss in $k_{cat}/K_{substrate}$ was due to substantial (up to 1000-fold) changes in k_{cat} (decrease) and $K_{substrate}$ (increase). k_{cat}/K for the coenzyme was also affected by the mutations, however, much less so than $k_{cat}/K_{substrate}$.

pH-dependencies and kinetic isotope effects

pH profiles of k_{cat} and $k_{cat}/K_{substrate}$ were determined for each of the singly mutated enzymes and are shown in a double-log plot (Figure 2) along with pH dependencies of relevant stopped-flow rate constants (k_{obs}) for wild-type PfM2DH. Determination of k_{obs} is described later. The pH dependencies of $k_{cat}/K_{mannitol}$ [20] and $k_{cat}/K_{fructose}$ [30] for the wild-type enzyme have been reported previously and are therefore not shown in Figure 2. However, relevant pK values from literature are shown in Table 2 to facilitate the comparison of native and mutated enzymes. N191A precipitated in the assay for mannitol oxidation at pH ≤ 6.5, restricting the investigatable pH range for this mutant. No k_{catO} values are available for N300A at pH ≤ 6.5 because saturation of the enzyme with mannitol was not achievable under these conditions. Fits of the data are displayed in Figure 2, and the resulting parameters are summarised in Table 2.

Licenced copy. Copying is not permitted, except with prior permission and as allowed by law.
© 2009 The Authors Journal compilation © 2009 Portland Press Limited

THIS IS NOT THE VERSION OF RECORD - see doi:10.1042/BJ20091441

Accepted Manuscript

Table S5 (see the Supplementary Information) displays ^{D}KIEs on kinetic parameters for each direction of reaction catalysed by mutated enzymes. This Table also shows the corresponding ^{D}KIEs on kinetic parameters for the wild-type enzyme [20, 30]. The ^{D2O}KIE on k_{catO} and $k_{cat}/K_{mannitol}$ for N191L was determined at pL 10.0, and values of 1.1 ± 0.1 and 3.6 ± 0.4 were obtained, respectively.

Transient kinetics

Figure 3 shows representative stopped-flow progress curves for mannitol oxidation and fructose reduction catalysed by wild-type and mutated enzymes. Reaction time courses for the wild-type PfM2DH in the pH range 7.1 – 10.0 were characterized by a transient burst of formation or consumption of NADH that was followed by the linear steady-state phase. Corresponding time courses for the mutated enzymes were linear (Figure 3), and the steady-state rate constants (k_{ss}) calculated from the data agreed very well with k_{cat} values obtained in conventional initial-rate measurements. We confirmed using wild-type PfM2DH and N191L that transient phase behaviour was independent of whether free enzyme or a pre-formed binary complex of enzyme and coenzyme (for N191L: enzyme-mannitol; see the Discussion) was rapidly mixed with the corresponding reactant solution (data not shown).

Despite the fact that ~90% and ~80% of the pre-steady burst in oxidation and reduction took place in the dead-time of the stopped-flow analyser, respectively, we were able to obtain reliable estimates for k_{obsO} and k_{obsR}, as described in detail in the Supplementary Results. k_{obsO} (at 25 °C and pH 10.0) was 1.5 (± 0.1) × 10^3 s^{-1} and k_{obsR} (at 25 °C and pH 7.1) was 4 (± 1) × 10^2 s^{-1}. The value for k_{obsO} was confirmed using analysis of the temperature dependence of the stopped-flow rate constant in the range 11 – 25 °C (see Supplementary Figure S4).

Figure 2 (panel A) shows that k_{obsR} was not pH dependent in the studied pH range. This result immediately suggests that the hydride transfer leading to oxidation of NADH by the wild-type enzyme is independent of pH, consistent with implications of a previous analysis of the pH dependence of $^{D}k_{cat}/K_{fructose}$ [30]. k_{obsO} by contrast displayed a decrease at low pH (Figure 2A). A fit of the pH profile with Eqn (1) yielded a pK of 6.8 (± 0.4). Take note of the change in pK for the pH dependence of k_{obsO} as compared to the pH dependence of $k_{cat}/K_{mannitol}$ (Table 2).

Transient kinetic analysis of proton release during enzymatic oxidation of mannitol

Supplementary Figure S5 shows stopped-flow progress curves for the decrease in bulk pH from its initial value of 8.0 during oxidation of mannitol by wild-type and N191L forms of PfM2DH. As expected from the stoichiometry of the overall reaction catalysed, D-mannitol + NAD^+ ←→ D-fructose + NADH + H^+, one mole proton was formed for each mole mannitol oxidised by either enzyme in the steady state. In the transient kinetic phase for wild-type PfM2DH, the change in total proton concentration corresponded to 1.7 ± 0.2 times the molar equivalent of enzyme present. Proton release was kinetically coupled to formation of 0.6 ± 0.1 moles NADH/mole enzyme in the pre-steady state, indicating that ~1.0 (= 1.7 – 0.6) mole proton/mole enzyme are not accounted for by the chemical reaction. Deprotonation of enzyme-NAD^+ as result of binding of mannitol explains release of "extra protons" in the reaction of the wild-type PfM2DH. N191L, by contrast, released only 0.45 ± 0.05 moles proton/mole enzyme rapidly. N300A did not release protons prior to formation of NADH in the stopped flow experiment at pH 8.0 (data not shown).

DISCUSSION

The degree of concertedness in the transfer of hydride and proton during enzymatic oxidation of alcohol by $NAD(P)^+$ determines the development of excess negative charge on oxygen, relative to carbon, in the course of the chemical reaction. The catalytic mechanism of Zn^{2+}-dependent ADH presents an extreme case where electrostatic stabilisation by the active-site

Licenced copy. Copying is not permitted, except with prior permission and as allowed by law.
© 2009 The Authors Journal compilation © 2009 Portland Press Limited

THIS IS NOT THE VERSION OF RECORD - see doi:10.1042/BJ20091441

Accepted Manuscript

metal promotes a stepwise transformation in which an alcoholate intermediate undergoes oxidation by hydride abstraction [23, 28, 29]. General base catalysis from a protein-derived group, as seen in various metal-independent ADHs [35, 36], would seem compatible with different levels of concertedness in the hydrogen transfer steps but is unlikely to facilitate a fully stepwise process. Evidence is presented here that establishes the oxyanion hole of PfM2DH as a novel structural motif for electrostatic stabilisation in ADH active sites. While we do not propose a completely developed oxyanion in PfM2DH as in Zn^{2+}-dependent ADH [23], partial abstraction of alcohol proton prior to hydride transfer presents an important catalytic factor in this enzyme and is facilitated by the residues of the binding pocket, Asn-191 and Asn-300.

Role of oxyanion hole residues for catalytic hydride transfer by PfM2DH

Observation of a pre-steady state burst of product formation in either direction of the reaction and the characteristic pattern of ^{D}KIEs where $^{D}k_{cat} < {}^{D}k_{cat}/K_{substrate}$ while $^{D}k_{cat}/K_{NAD(H)} \approx 1$ supports previous evidence [20, 30] suggesting that in wild-type PfM2DH, dissociation of the second product, NADH or NAD^+, controls the rates (k_{cat}) of mannitol oxidation or fructose reduction at the respective optimum pH of 10.0 and 7.1. Transient kinetic data further show that proton exchange with solvent as result of the chemical reaction occurs prior to the rate-limiting dissociation of coenzyme. Elimination of "burst kinetics" in the mutated enzymes together with the finding that $^{D}k_{cat}$ was now equal to $^{D}k_{cat}/K_{substrate}$ clearly locates rate limitation in their catalytic steps. Comparison of k_{obs} (wild-type) and k_{cat} (or k_{ss}; single point mutants) reveals that each site-directed replacement resulted in a drastic ($5 \times 10^2 - 3 \times 10^3$-fold) impaired reaction rate constant. It is interesting that a decrease in k_{obs} as large as this was not accompanied by a significant unmasking of the hydride transfer step, detectable as increase in $^{D}k_{cat}/K_{substrate}$ for the mutated enzymes as compared to the corresponding ^{D}KIE for wild-type PfM2DH (see Table S5). A plausible explanation is that substitution of either Asn in the oxyanion hole not only affects the actual hydride transfer but it also causes slowing down of the isomerisation step (k_3 and k_4 in Scheme 1B) that precedes catalysis in the oxidation direction.

Using the relationships $\Delta\Delta G_T^{\ddagger} = -RT \ln[(k_{cat}/K_{susbtrate})^{mutant} / (k_{cat}/K_{substrate})^{wild\text{-}type}]$ and $\Delta\Delta G^{\ddagger} = -RT \ln[k_{cat}^{mutant} / k_{obs}^{wild\text{-}type}]$, catalytic defects resulting from replacement of one or both asparagines can be expressed as losses in transition state-stabilising energy ($\Delta\Delta G_T^{\ddagger}$) and activation free energy for the reaction ($\Delta\Delta G^{\ddagger}$). The calculated $\Delta\Delta G_T^{\ddagger}$ values (see Supplementary Table S6) for Asn→Ala mutants were similar and additive in the doubly mutated enzyme N191A-N300A, suggesting that Asn-191 and Asn-300 act independently one from another in promoting NAD(H)-dependent interconversion of mannitol and fructose (Figure 1) (for the general case, see ref. [37]). The finding that $\Delta\Delta G_T^{\ddagger} \approx \Delta\Delta G^{\ddagger}$ (see Supplementary Table S6) implies that the disruptive effect of individual substitutions of Asn-191 and Asn-300 was predominantly on the catalytic steps, with substrate binding being less strongly affected. The magnitude of the observed changes in Gibbs free energy caused by the mutations is consistent with the expected net effect of removing a hydrogen bond to a charged donor / acceptor group [38, 39] and thus supports a function of Asn-191 and Asn-300 as oxyanion stabilisers.

In the ordered kinetic mechanism of wild-type PfM2DH where binding of coenzyme precedes the binding of substrate in either direction of the reaction [20], k_{cat}/K_m for NAD^+ and NADH are the bimolecular rate constants describing formation of the respective enzyme-coenzyme complex. The pattern of ^{D}KIEs associated with this kinetic mechanism is $^{D}k_{cat}/K_{substrate} > 1$ and $^{D}k_{cat}/K_{NAD(H)} = 1$ (for the general case, see [40]). In the mutants (N191A, N191L), this pattern was changed to $^{D}k_{cat}/K_{substrate} \approx {}^{D}k_{cat}/K_{NAD^+} \approx {}^{D}k_{cat} > 1$, inconsistent with strictly ordered substrate binding, NAD^+ prior to mannitol. These ^{D}KIEs would suggest a rapid equilibrium mechanism or a steady-state random mechanism for the two mutated enzymes in which the off rates for both NAD^+ and mannitol from enzyme-NAD^+-mannitol are

Licenced copy. Copying is not permitted, except with prior permission and as allowed by law.
© 2009 The Authors Journal compilation © 2009 Portland Press Limited

THIS IS NOT THE VERSION OF RECORD - see doi:10.1042/BJ20091441

Accepted Manuscript

equal [40]. Because the binary complex with mannitol is allowed in the reaction of the mutants, k_{cat}/K_m for NAD^+ determined in the presence of a saturating substrate concentration can be sensitive to site-directed substitution despite the fact that neither Asn-191 nor Asn-300 appear to be required for binding of NAD^+ to the free enzyme (K_d).

Mechanistic deductions from pH dependencies of rate constants and their ^{D}KIEs

Because mannitol and fructose do not ionise in the pH range studied, only protonation/deprotonation equilibria for the enzyme are considered in the interpretation of pH effects on rates and ^{D}KIEs. Therefore, pH dependencies of $k_{cat}/K_{mannitol}$ and $k_{cat}/K_{fructose}$ reveal ionisations in enzyme-NAD^+ and enzyme-NADH, respectively, while pH dependencies of k_{obs} (wild-type enzyme) and k_{cat} (mutants) show ionisations of the respective ternary complexes.

The low pK of 6.8 observed in the pH profile of logk_{obsO} suggests that upon binding of mannitol to enzyme-NAD^+ in wild-type PfM2DH, the pK of Lys-295 undergoes a large shift by 2.5 (= 9.2 – 6.8) pH units toward the acidic range. Rapid mixing of enzyme-NAD^+ with mannitol at pH 8.0 where Lys-295 (pK = 9.2) should be largely (94%) protonated was accompanied by the immediate release of one proton from the enzyme, fully consistent with the proposed pK depression in response to binding of alcohol substrate. Using N191L, proton release upon binding of mannitol at pH 8.0 corresponded to only half the molar equivalent of enzyme present, as expected from the pH profile of logk_{catO}, suggesting a pK of 8.0 for Lys-295 in N191L-NAD^+-mannitol. The absence of transient proton release by N300A is consistent with the pH-logk_{catO} dependence, suggesting that at pH 8.0, only a small fraction of N300A-NAD^+-mannitol is in the correct protonation state for reaction.

k_{obsR} for wild-type PfM2DH was invariant within the pH span 7.1 – 10.0, probably indicating that binding of fructose caused a shift in pK for Lys-295, from 9.2 in enzyme-NADH to a higher value that was out of the measured range. The large difference in pK for Lys-295 in ternary complexes undergoing oxidation (pK = 6.8) and reduction (pK > 10) is remarkable. An interesting question raised by the high pK of Lys-295 in enzyme-fructose-NADH is which enzyme group eventually releases the proton formed during oxidation of mannitol by NAD^+. We have preliminary evidence that a mobile Glu-292 situated in the water channel that connects Lys-295 with bulk solvent [16] might be responsible (M.K. and B.N., unpublished results 2009).

The pH dependencies of $k_{cat}/K_{substrate}$ for the mutated enzymes where (logarithmic) oxidation rates increased linearly as the pH was raised and reduction rates did not vary within the pH range studied are consistent with a substantial increase in pK for Lys-295 in enzyme-NAD^+ as well as enzyme-NADH, relative to the pK of the Lys in the corresponding native complexes, as result of the site-directed replacements. The alternative interpretation that specific Brønsted catalysis by hydroxide and water facilitate oxidation and reduction in the mutants, respectively, appears inconsistent with the low ^{D2O}KIE on k_{catO} for N191L [26]. Comparison of pK values from pH profiles of logk_{catO} (mutants) and logk_{obsO} (wild-type enzyme) support the notion of pK elevation for Lys-295 in the ternary complex in response to substitution of Asn-191 and Asn-300. Note: partial retention of activity in N191L at low pH (k_{catO}, $k_{catO}/K_{mannitol}$) is not explained by the mechanism proposed and was not further pursued in the course of this work.

The pH dependencies of the ^{D}KIEs on $k_{cat}/K_{substrate}$ for oxidation and reduction catalysed by native PfM2DH suggested a mechanism (Scheme 1B) where the group comprising the reactive groups of mannitol and Lys-295 loses a proton (as H_2O) at high pH (≥ 10.5) [20]. The commitment of the enzyme-substrate complex to catalysis becomes infinite upon deprotonation, causing the ^{D}KIE on hydride transfer to be completely masked in the measured value of $^Dk_{catO}/K_{mannitol}$ (= 1.00). The equilibrium ^{D}KIE (0.85) is seen on $k_{catR}/K_{fructose}$ because proton uptake is effectively prevented under these conditions. The absence of a similar pH dependence of $^Dk_{cat}/K_{substrate}$ for single-site mutants of PfM2DH in the measured pH range

Licenced copy. Copying is not permitted, except with prior permission and as allowed by law.
© 2009 The Authors Journal compilation © 2009 Portland Press Limited

THIS IS NOT THE VERSION OF RECORD - see doi:10.1042/BJ20091441

Accepted Manuscript

indicates that either deprotonation of the relevant ionisable group does not occur or its p*K* is shifted to a higher pH once the oxyanion hole has been partially disrupted.

Proposed function of Asn-191 and Asn-300 in catalysis

This work delineates two important roles fulfilled by the oxyanion hole of PfM2DH in enzymatic catalysis to NAD(H)-dependent interconversion of mannitol and fructose (Scheme 2). The first role is activation of the catalytic base function of Lys-295 through suitable p*K* depression in enzyme-NAD^+-mannitol. A pH-dependent conformational equilibrium, also identified in other metal-independent dehydrogenases [35] and choline oxidase [41], locks the ternary complex in the ionisation state for mannitol oxidation. Asn-191 and Asn-300 are key to these pre-catalytic steps, and they also determine ionisations observed in binary and ternary enzyme-substrate complexes (Schemes 1B and 2). Mutation of either Asn-191 and Asn-300 therefore disrupts the enzyme active site of its ability to finely tune the p*K* of Lys-295. While it stands to reason that binding of fructose results in an increased p*K* for Lys-295, it is not immediately obvious why hydrogen bonding to the carboxamide oxygens of Asn-191 and Asn-300 (Scheme 2) should stabilise the protonated ε-amino group of the lysine in enzyme-NAD^+ and enzyme-NADH, as implied by the effects of partial disruption of the oxyanion hole on the pH dependencies of $k_{cat}/K_{substrate}$. However, the crystal structure of wild-type enzyme bound to NAD^+ [16] suggests that the side chain of Lys-295 relays its proton via active-site water to Glu-292, the main candidate residue for proton transfer to bulk solvent. A plausible scenario therefore is that "pull" by the proton shuttle system causes p*K* depression in Lys-295 and that the oxyanion hole is required to position Lys-295 for efficient proton relay.

The second role of the oxyanion hole, supported by KIEs and pH dependencies thereof, is activation of the reactive substrate group and stabilisation of the emerging negative charge on oxygen in the pre-catalytic conformers for oxidation and reduction (Scheme 2). In the proposed mechanism, partial abstraction of the proton from the 2-OH group of mannitol to Lys-295 is aided by the oxyanion hole dipoles and renders the substrate competent for subsequent hydride transfer. In the direction of fructose reduction, the reactive carbonyl group becomes polarised through the interaction of its oxygen with the side-chains of Asn-191 and Asn-300. Finally, electrostatic contacts are tightened in the hydride transfer step where they contribute about 40 kJ/mol of stabilisation energy.

In addition to the unprecedented use of a protease-like oxyanion hole for electrostatic stabilisation in an ADH active site, structure-function relationships for PfM2DH are also relevant in showing that the task of a pre-catalytic alcohol activation fulfilled by Lys-295, Asn-191 and Asn-300 is strikingly similar to that of active-site zinc in ADHs of the medium-chain dehydrogenase/reductase type [6]. Family-wide conservation of the PfM2DH triad of residues suggests that this “protein-derived functional mimic of zinc” is a common catalytic feature for PSLDRs [24, 25].

ACKNOWLEDGEMENTS

We thank Veronika Milocco and Valentin Pacher for expert technical assistance. Professor Walter Keller (Institute of Molecular Biosciences, University of Graz, Austria) is thanked for assistance during recording CD spectra.

THIS IS NOT THE VERSION OF RECORD - see doi:10.1042/BJ20091441

Accepted Manuscript

Licenced copy. Copying is not permitted, except with prior permission and as allowed by law.
© 2009 The Authors Journal compilation © 2009 Portland Press Limited

THIS IS NOT THE VERSION OF RECORD - see doi:10.1042/BJ20091441

Accepted Manuscript

REFERENCES

1 Silverman, R. B. (2002) Mechanisms of enzyme catalysis. In The organic chemistry of enzyme-catalyzed reactions (Silverman, R. B., ed.). pp. 15-30, Academic Press, San Diego

2 Anderson, V. E., Ruszczycky, M. W. and Harris, M. E. (2006) Activation of oxygen nucleophiles in enzyme catalysis. Chem. Rev. **106**, 3236-3251

3 Fersht, A. (1998) Chemical catalysis. In Structure and mechanism in protein science: a guide to enzyme catalysis and protein folding (Fersht, A., ed.). pp. 54-102, W. H. Freeman and Company, New York

4 Ghanem, M. and Gadda, G. (2005) On the catalytic role of the conserved active site residue His466 of choline oxidase. Biochemistry **44**, 893-904

5 Hedstrom, L. (2002) Serine protease mechanism and specificity. Chem. Rev. **102**, 4501-4524

6 Meijers, R. and Cedergren-Zeppezauer, E. (2004) Zinc dependent medium-chain dehydrogenases/reductases. In Handbook of metalloproteins (Messerschmidt, W. B., Bode, W. and Cygler, M., eds.). pp. 5-33, Wiley, Chichester

7 Vendrell, J., Aviles, F. X. and Fricker, L. D. (2004) Metallocarboxypeptidases. In Handbook of metalloproteins (Messerschmidt, W. B., Bode, W. and Cygler, M., eds.), Wiley, Chichester

8 Warshel, A., Sharma, P. K., Kato, M., Xiang, Y., Liu, H. and Olsson, M. H. (2006) Electrostatic basis for enzyme catalysis. Chem. Rev. **106**, 3210-3235

9 Henderson, R. (1970) Structure of crystalline α-chymotrypsin: IV. The structure of indoleacryloyl-α-chyotrypsin and its relevance to the hydrolytic mechanism of the enzyme. J. Mol. Biol. **54**, 341-354

10 Warshel, A., Naray-Szabo, G., Sussman, F. and Hwang, J. K. (1989) How do serine proteases really work? Biochemistry **28**, 3629-3637

11 Bhatnagar, R. S., Fütterer, K., Farazi, T. A., Korolev, S., Murray, C. L., Jackson-Machelski, E., Gokel, G. W., Gordon, J. I. and Waksman, G. (1998) Structure of N-myristoyltransferase with bound myristoylCoA and peptide substrate analogs. Nat. Struct. Biol. **5**, 1091-1097

12 Birktoft, J. J. and Blow, D. M. (1972) Structure of crystalline -chymotrypsin. V. The atomic structure of tosyl- -chymotrypsin at 2 Å resolution. J. Mol. Biol. **68**, 187-240

13 Cobessi, D., Tête-Favier, F., Marchal, S., Branlant, G. and Aubry, A. (2000) Structural and biochemical investigations of the catalytic mechanism of an NADP-dependent aldehyde dehydrogenase from *Streptococcus mutans*. J. Mol. Biol. **300**, 141-152

14 Eschenburg, S., Genov, N., Peters, K., Fittkau, S., Stoeva, S., Wilson, K. S. and Betzel, C. (1998) Crystal structure of subtilisin DY, a random mutant of subtilisin Carlsberg. Eur. J. Biochem. **257**, 309-318

15 Janowski, R., Kozak, M., Jankowska, E., Grzonka, Z. and Jaskolski, M. (2004) Two polymorphs of a covalent complex between papain and a diazomethylketone inhibitor. J. Pept. Res. **64**, 141-150

16 Kavanagh, K. L., Klimacek, M., Nidetzky, B. and Wilson, D. K. (2002) Crystal structure of *Pseudomonas fluorescens* mannitol 2-dehydrogenase binary and ternary complexes. Specificity and catalytic mechanism. J. Biol. Chem. **277**, 43433-43442

17 Kursula, I., Partanen, S., Lambeir, A. M., Antonov, D. M., Augustyns, K. and Wierenga, R. K. (2001) Structural determinants for ligand binding and catalysis of triosephosphate isomerase. Eur. J. Biochem. **268**, 5189-5196

18 D'Ambrosio, K., Pailot, A., Talfournier, F., Didierjean, C., Benedetti, E., Aubry, A., Branlant, G. and Corbier, C. (2006) The first crystal structure of a thioacylenzyme intermediate in the ALDH family: new coenzyme conformation and relevance to catalysis. Biochemistry **45**, 2978-2986

Licenced copy. Copying is not permitted, except with prior permission and as allowed by law.
© 2009 The Authors Journal compilation © 2009 Portland Press Limited

19 Farazi, T. A., Waksman, G. and Gordon, J. I. (2001) Structures of *Saccharomyces cerevisiae* N-myristoyltransferase with bound myristoylCoA and peptide provide insights about substrate recognition and catalysis. Biochemistry **40**, 6335-6343

20 Klimacek, M. and Nidetzky, B. (2002) Examining the relative timing of hydrogen abstraction steps during NAD^+-dependent oxidation of secondary alcohols catalyzed by long-chain D-mannitol dehydrogenase from *Pseudomonas fluorescens* using pH and kinetic isotope effects. Biochemistry **41**, 10158-10165

21 Agarwal, P. K., Webb, S. P. and Hammes-Schiffer, S. (2000) Computational studies of the mechanism for proton and hydride transfer in liver alcohol dehydrogenase. J. Am. Chem. Soc. **112**, 4803-4812

22 Pettersson, G. (1987) Liver alcohol dehydrogenase. CRC critical reviews in biochemistry **21**, 349-389

23 Ramaswamy, S., Park, D. H. and Plapp, B. V. (1999) Substitutions in a flexible loop of horse liver alcohol dehydrogenase hinder the conformational change and unmask hydrogen transfer. Biochemistry **38**, 13951-13959

24 Klimacek, M., Kavanagh, K. L., Wilson, D. K. and Nidetzky, B. (2003) *Pseudomonas fluorescens* mannitol 2-dehydrogenase and the family of polyol-specific long-chain dehydrogenases/reductases: sequence-based classification and analysis of structure-function relationships. Chem. Biol. Interact. **143-144**, 559-582

25 Nidetzky, B. and Klimacek, M. (2007) Fungal mannitol 2-dehydrogenases and mannitol-1-phosphate 5-dehydrogenases constitutes novel branches in the protein family of polyol-specific long-chain dehydrogenases and reductases. In Enzymology and molecular biology of carbonyl metabolism 13 (Weiner, H., Maser, E., Lindahl, R. and Plapp, B. V., eds.). pp. 305-322, Purdue University Press, West Lafayette, Indiana

26 Klimacek, M., Kavanagh, K. L., Wilson, D. K. and Nidetzky, B. (2003) On the role of Brønsted catalysis in *Pseudomonas fluorescens* mannitol 2-dehydrogenase. Biochem. J. **375**, 141-149

27 Klimacek, M. and Nidetzky, B. (2002) A catalytic consensus motif for D-mannitol 2-dehydrogenase, a member of a polyol-specific long-chain dehydrogenase family, revealed by kinetic characterization of site-directed mutants of the enzyme from *Pseudomonas fluorescens*. Biochem. J. **367**, 13-18

28 Cook, P. F. and Cleland, W. W. (1981) pH variation of isotope effects in enzyme-catalyzed reactions. 2. Isotope-dependent step not pH dependent. Kinetic mechanism of alcohol dehydrogenase. Biochemistry **20**, 1805-1816.

29 Kvassman, J. and Pettersson, G. (1980) Unified mechanism for proton-transfer reactions affecting the catalytic activity of liver alcohol dehydrogenase. Eur. J. Biochem. **103**, 565-575

30 Slatner, M., Nidetzky, B. and Kulbe, K. D. (1999) Kinetic study of the catalytic mechanism of mannitol dehydrogenase from *Pseudomonas fluorescens*. Biochemistry **38**, 10489-10498

31 Ellis, K. J. and Morrison, J. F. (1982) Buffers of constant ionic strength for studying pH-dependent processes. Methods Enzymol. **87**, 405-426

32 Northrop, D. B. (1977) Determining the absolute magnitude of hydrogen isotope effects. In Isotope effects on enzyme-catalyzed reactions (Cleland, W. W., O'Leary, M. H. and Northrop, D. B., eds.). p. 122, University Park Press, Baltimore, MD

33 Klimacek, M., Hellmer, H. and Nidetzky, B. (2007) Catalytic mechanism of Zn^{2+}-dependent polyol dehydrogenases: kinetic comparison of sheep liver sorbitol dehydrogenase with wild-type and Glu154-->Cys forms of yeast xylitol dehydrogenase. Biochem. J. **404**, 421-429

34 Cook, P. F. and Cleland, W. W. (1981) Mechanistic deductions from isotope effects in multireactant enzyme mechanisms. Biochemistry **20**, 1790-1796.

THIS IS NOT THE VERSION OF RECORD - see doi:10.1042/BJ20091441

Accepted Manuscript

Licenced copy. Copying is not permitted, except with prior permission and as allowed by law.
© 2009 The Authors Journal compilation © 2009 Portland Press Limited

35 Hwang, C. C. and Cook, P. F. (1998) Multiple isotope effects as a probe of proton and hydride transfer in the 6-phosphogluconate dehydrogenase reaction. Biochemistry **37**, 15698-15702

36 Filling, C., Berndt, K. D., Benach, J., Knapp, S., Prozorovski, T., Nordling, E., Ladenstein, R., Jörnvall, H. and Oppermann, U. (2002) Critical residues for structure and catalysis in short-chain dehydrogenases/reductases. J. Biol. Chem. **277**, 25677-25684

37 Mildvan, A. S. (2004) Inverse thinking about double mutants of enzymes. Biochemistry **43**, 14517-14520

38 Bryan, P., Pantoliano, M. W., Quill, S. G., Hsiao, H. Y. and Poulos, T. (1986) Site-directed mutagenesis and the role of the oxyanion hole in subtilisin. Proc. Natl. Acad. Sci. U. S. A. **83**, 3743-3745

39 Fersht, A. (1987) The hydrogen bond in molecular recognition. Trends Biochem. Sci. **12**, 301-304

40 Cook, P. F. (1991) pH dependence of isotope effects in enzyme catalyzed reactions. In Enzyme mechanism form isotope effects (Cook, P. F., ed.). pp. 231-246, CRC Press, Boca Raton

41 Fan, F. and Gadda, G. (2005) On the catalytic mechanism of choline oxidase. J. Am. Chem. Soc. **127**, 2067-2074

42 Collins, P. and Ferrier, R. (1995) Monosaccharides: Their Chemistry and Their Roles in Natural Products. Wiley, Chichester

THIS IS NOT THE VERSION OF RECORD - see doi:10.1042/BJ20091441

Accepted Manuscript

Licenced copy. Copying is not permitted, except with prior permission and as allowed by law.
© 2009 The Authors Journal compilation © 2009 Portland Press Limited

FIGURE LEGENDS

Figure 1. Arrangement of catalytic and reactive groups in the active site of PfM2DH. X-ray co-ordinates for enzyme bound with NAD^+ and mannitol (PDB 1M2W) were used [16]. Distances are in Å.

Figure 2. pH profiles of logk_{cat} (A) and log($k_{cat}/K_{substrate}$) (B) for mutated PfM2DHs and of logk_{obs} (A) for wild-type enzyme. Closed and open symbols indicate mannitol oxidation and fructose reduction, respectively. Symbols: circles, N191L; triangles up, N191A; squares, N300A; triangles down, logk_{obs} of wild-type PfM2DH. Non-linear or linear fits to the data are shown as solid lines. A trend line for logk_{catO} of N191A is displayed as this parameter did not level out in the measured pH range. The linear fit of the pH dependence of log($k_{catO}/K_{substrate}$) for N191L was performed in the pH range 7.1 – 10.5.

Figure 3. Multiple turnover stopped-flow progress curves for mannitol oxidation and fructose reduction catalysed by wild-type PfM2DH (A and C) and mutants thereof (B and D). Dark traces are the measured curves (panels A and C) and lines (panels B and D) whereas grey lines show fits of Eqn S2 (mannitol oxidation) and Eqn S3 (fructose reduction) to the data. Stopped-flow traces obtained in relevant control experiments (lacking the enzyme) are also shown and reveal the stability of the absorbance measurement. Details of the reaction conditions are summarised in Supplementary Tables S2 and S3 (panel A: D1, D4; panel B: E4, F2, G2, E5, F3, G3; panel C: A2, A3; panel D: E3, F1, G1).

Scheme 1. (A) Proposed catalytic stabilisation by residues of the oxyanion hole in PfM2DH and (B) kinetic mechanism describing the pH dependence of NAD(H)-dependent interconversion of mannitol and fructose by the enzyme [20]. (A) Only the reactive part of mannitol is shown for reasons of clarity. (B) Formation of a fully developed alkoxide is tentative.

Scheme 2. Proposed participation of the oxyanion hole in the catalytic mechanism of PfM2DH. The indicated p*K* values are the ionisations shown in Scheme 1B. The ternary complex of enzyme, NAD^+ and mannitol becomes "activated" for undergoing reaction through (partial) abstraction of the hydroxyl proton of mannitol by the ε-NH_2 nitrogen of Lys-295. Non-covalent bonds in bold indicate tightened interactions upon moving from the reactant states to the transition state (TS). Only the reactive parts of mannitol, fructose and NAD(H) are drawn for clarity reasons.

THIS IS NOT THE VERSION OF RECORD - see doi:10.1042/BJ20091441

Accepted Manuscript

Licenced copy. Copying is not permitted, except with prior permission and as allowed by law.
© 2009 The Authors Journal compilation © 2009 Portland Press Limited

TABLES

Table 1. Kinetic parameters for site-directed mutants of PfM2DH. Parameters of the wild-type enzyme are shown as reference. [a]Mannitol oxidation at pH 10.0 and fructose reduction at pH 7.1; [b]Parameters for mannitol oxidation are from reference [20]; [c]Michaelis constant obtained at a constant, non-saturating concentration of mannitol (1.00 M); [d]Determined by fluorescence titration [27]; [e]Values obtained at a constant, non-saturating concentration of fructose (2.00 M); [f]Values corrected for the portion (1%) of free carbonyl form present in aqueous solution of fructose [42]

Parameter[a]	Wild type[b]	N191L	N300A[b]	N191A	N191A/N300A
k_{catO} [s^{-1}]	40.0 ± 0.5	0.55 ± 0.01	2.61 ± 0.02	2.78 ± 0.01	0.04 ± 0.01
$K_{mannitol}$ [mM]	0.40 ± 0.02	0.9 ± 0.1	26 ± 1	8.7 ± 0.5	1187 ± 208
K_{NAD^+} [μM]	93 ± 8	55 ± 2	25 ± 3	310 ± 20	314 ± 12[c]
$k_{cat}/K_{mannitol}$ [$M^{-1}s^{-1}$]	1.0×10^5	598	98.9	319	0.034
k_{cat}/K_{NAD^+} [$M^{-1}s^{-1}$]	4.0×10^5	9964	1.0×10^5	8968	127.4
K_{dNAD^+} [μM][d]	1200 ± 45	859 ± 30	835 ± 53	990 ± 52	760 ± 80
k_{catR} [s^{-1}]	61 ± 1.5	0.55 ± 0.01	0.45 ± 0.01	0.56 ± 0.02	$> 4.5 \times 10^{-4} \pm 2 \times 10^{-5}$ [e]
$K_{fructose}$ [mM][f]	0.24 ± 0.03	1.1 ± 0.1	4.2 ± 0.3	9 ± 1	> 20
K_{NADH} [μM]	67 ± 4	3.3 ± 0.4	12.5 ± 0.5	17 ± 1	23 ± 3[e]
$k_{cat}/K_{fructose}$ [$M^{-1}s^{-1}$][f]	2.5×10^5	407.4	108.4	64.2	0.026
k_{cat}/K_{NADH} [$M^{-1}s^{-1}$]	9.1×10^5	1.7×10^5	3.6×10^4	3.2×10^4	> 19.4[e]

THIS IS NOT THE VERSION OF RECORD - see doi:10.1042/BJ20091441

Accepted Manuscript

Licenced copy. Copying is not permitted, except with prior permission and as allowed by law.
© 2009 The Authors Journal compilation © 2009 Portland Press Limited

Table 2. Results from pH studies. [a] Ionisation constants from references [20, 30]. [b] C is the pH-independent value of the respective kinetic parameter. C_L and C_H are the pH-independent values of k_{catO} at low and high pH, respectively.

Enzyme	Parameter	p*K*	C[b] [s^{-1}]; [$s^{-1}M^{-1}$]	Eqn	r^2
Wild type	k_{obsR}	p*K* > 10.0			
	k_{obsO}	p*K* = 6.8 ± 0.4	1580 ± 75	1	0.80
	$k_{cat}/K_{mannitol}$	p*K* = 9.2 ± 0.1[a]			
	$k_{cat}/K_{fructose}$	p*K* = 9.2 ± 0.1[a]			
N191A	k_{catO}	p*K* > 10.5			
N191L	k_{catO}	p*K* = 8.0 ± 0.1	C_L = 0.077 ± 0.004 C_H = 0.62 ± 0.02	2	0.99
N300A	k_{catO}	pK_1 = 8.3 ± 0.3			
		pK_2 = 8.7 ± 0.4	2.7 ± 0.1	3	0.995
		pK_3 = 6.7 ± 0.2			

THIS IS NOT THE VERSION OF RECORD - see doi:10.1042/BJ20091441

Accepted Manuscript

Licenced copy. Copying is not permitted, except with prior permission and as allowed by law.
© 2009 The Authors Journal compilation © 2009 Portland Press Limited

FIGURES AND SCHEMES

Figure 1

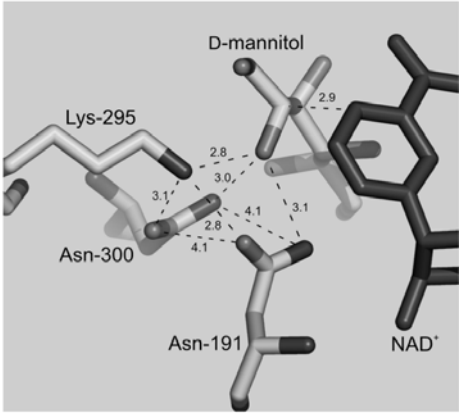

THIS IS NOT THE VERSION OF RECORD - see doi:10.1042/BJ20091441

Accepted Manuscript

Licenced copy. Copying is not permitted, except with prior permission and as allowed by law.
© 2009 The Authors Journal compilation © 2009 Portland Press Limited

Figure 2

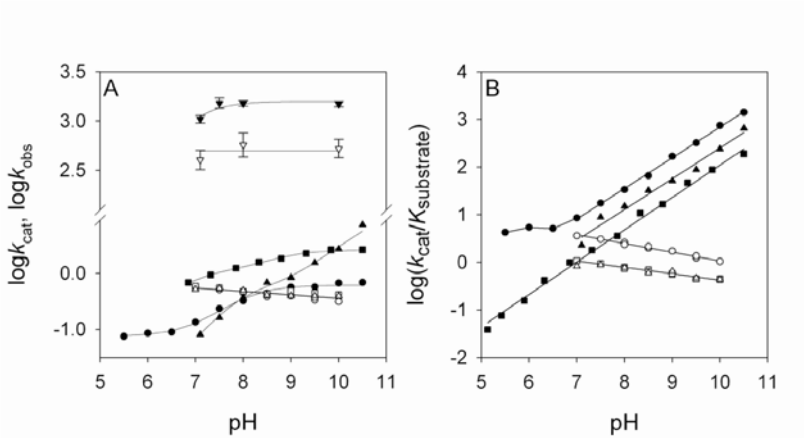

THIS IS NOT THE VERSION OF RECORD - see doi:10.1042/BJ20091441

Accepted Manuscript

Licenced copy. Copying is not permitted, except with prior permission and as allowed by law.
© 2009 The Authors Journal compilation © 2009 Portland Press Limited

Figure 3

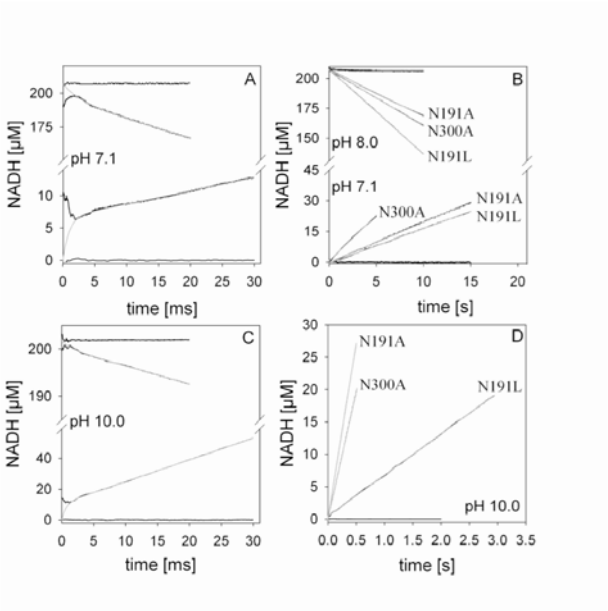

THIS IS NOT THE VERSION OF RECORD - see doi:10.1042/BJ20091441

Accepted Manuscript

Licenced copy. Copying is not permitted, except with prior permission and as allowed by law.
© 2009 The Authors Journal compilation © 2009 Portland Press Limited

Scheme 1

A

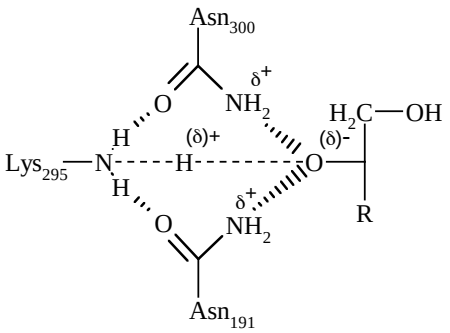

B

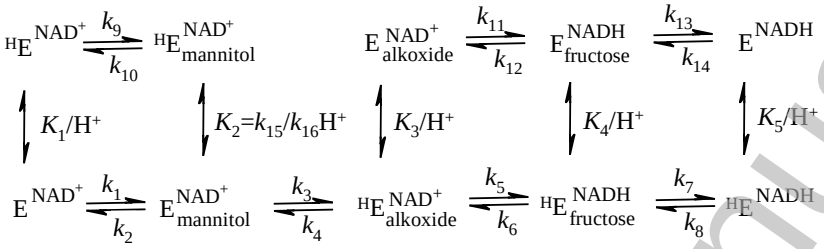

THIS IS NOT THE VERSION OF RECORD - see doi:10.1042/BJ20091441

Accepted Manuscript

Licenced copy. Copying is not permitted, except with prior permission and as allowed by law.
© 2009 The Authors Journal compilation © 2009 Portland Press Limited

Scheme 2

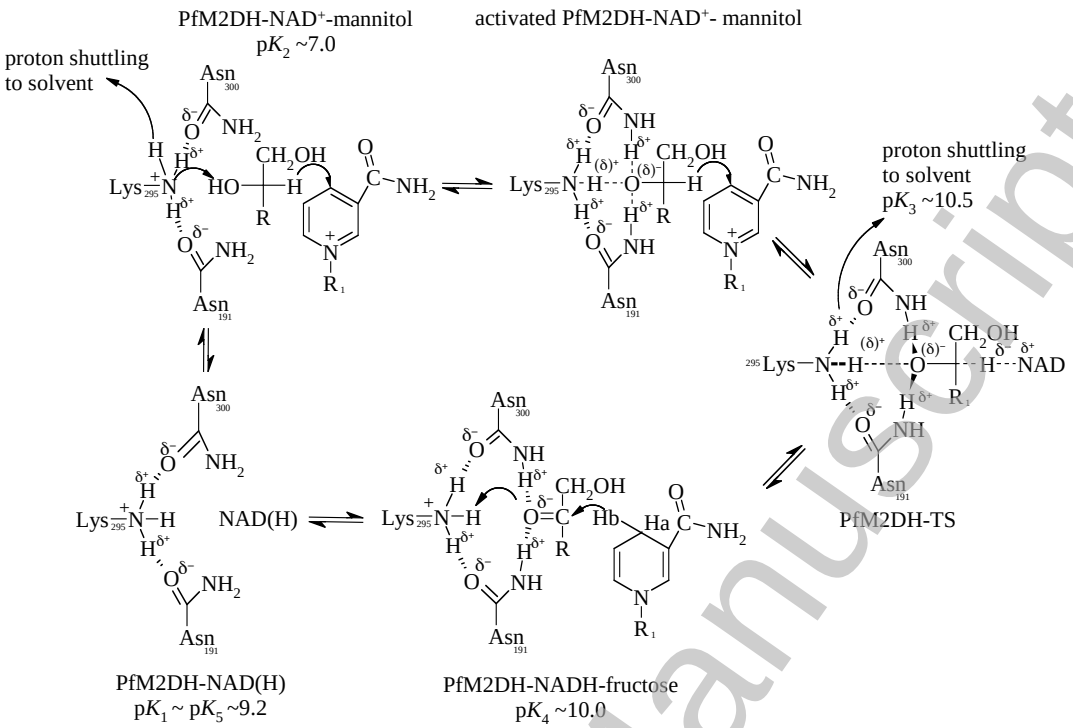

THIS IS NOT THE VERSION OF RECORD - see doi:10.1042/BJ20091441

Accepted Manuscript

Licenced copy. Copying is not permitted, except with prior permission and as allowed by law.
© 2009 The Authors Journal compilation © 2009 Portland Press Limited